

PROCEEDINGS OF SPIE

[SPIDigitalLibrary.org/conference-proceedings-of-spie](https://spiedigitallibrary.org/conference-proceedings-of-spie)

VIRUS: status and performance of the massively-replicated fiber integral field spectrograph for the upgraded Hobby-Eberly Telescope

Gary J. Hill, Andreas Kelz, Hanshin Lee, Phillip MacQueen, Trent W. Peterson, et al.

Gary J. Hill, Andreas Kelz, Hanshin Lee, Phillip MacQueen, Trent W. Peterson, Jason Ramsey, Brian L. Vattiat, D. L. DePoy, Niv Drory, Karl Gebhardt, John M. Good, Thomas Jahn, Herman Kriel, J. L. Marshall, Sarah E. Tuttle, Greg Zeimann, Edmundo Balderrama, Randy Bryant, Brent Buetow, Taylor S. Chonis, George Damm, Maximilian H. Fabricius, Daniel Farrow, James R. Fowler, Cynthia Froning, Dionne M. Haynes, Briana L. Indahl, Jerry Martin, Francesco Montesano, Emily Mrozinski, Harald Nicklas, Eva Noyola, Stephen Odewahn, Andrew Peterson, Travis Prochaska, Sergey Rostopchin, Matthew Shetrone, Greg Smith, Jan M. Snigula, Renny Spencer, Amy Westfall, Taft Armandroff, Ralf Bender, Gavin Dalton, Matthias Steinmetz, "VIRUS: status and performance of the massively-replicated fiber integral field spectrograph for the upgraded Hobby-Eberly Telescope," Proc. SPIE 10702, Ground-based and Airborne Instrumentation for Astronomy VII, 107021K (6 July 2018); doi: 10.1117/12.2314280

SPIE.

Event: SPIE Astronomical Telescopes + Instrumentation, 2018, Austin, Texas, United States

VIRUS: status and performance of the massively-replicated fiber integral field spectrograph for the upgraded Hobby-Eberly Telescope^{*}

Gary J. Hill^{a,b†}, Andreas Kelz^{c,d}, Hanshin Lee^a, Phillip MacQueen^a, Trent W. Peterson^a, Jason Ramsey^a, Brian L. Vattiat^a, D.L. DePoy^e, Niv Drory^a, Karl Gebhardt^b, John M. Good^a, Thomas Jahn^{c,d}, Herman Kriel^f, J.L. Marshall^e, Sarah E. Tuttle^g, Greg Zeimann^{a,f}, Edmundo Balderrama^f, Randy Bryant^f, Brent Buetow^f, Taylor Chonis^h, George Damm^f, Maximilian H. Fabricius^{ij}, Daniel Farrowⁱ, Jim Fowler^f, Cynthia Froning^a, Dionne M. Haynes^{c,d}, Briana L. Indahl^b, Jerry Martin^f, Francesco Montesanoⁱ, Emily Mrozinski^f, Harald Nicklas^k, Eva Noyola^a, Stephen Odewahn^f, Andrew Peterson^a, Travis Prochaska^e, Sergey Rostopchin^f, Matthew Shetrone^f, Greg Smith^f, Jan M. Snigula^{ij}, Renny Spencer^f, Amy Westfall^f, Taft Armandroff^{a,b}, Ralf Bender^{ij}, Gavin Dalton^l, & Matthias Steinmetz^c

^a McDonald Observatory, ^b Department of Astronomy, University of Texas at Austin, 2515 Speedway, Austin, TX 78712, USA

^c Leibniz Institute for Astrophysics (AIP), ^d innoFSPEC Potsdam, An der Sternwarte 16, 14482 Potsdam, Germany

^e Department of Physics and Astronomy, Texas A&M University, College Station, TX 77843, USA

^f Hobby-Eberly Telescope, 82 Mt. Locke Rd., McDonald Observatory, TX 79734, USA

^g Department of Astronomy, University of Washington, Seattle, WA 98195, USA

^h Ball Aerospace, Boulder, CO, USA

ⁱ Max-Planck-Institut für Extraterrestrische-Physik, Giessenbachstrasse, D-85748 Garching b. München, Germany

^j Universitäts-Sternwarte München, Scheinerstr. 1, 81679 München, Germany

^k Institut für Astrophysik Göttingen, Friedrich-Hund-Platz 1, 37077 Göttingen, Germany

^l Department of Physics, Oxford University, Keble Road, Oxford, OX1 3RH, UK

ABSTRACT

The Visible Integral-field Replicable Unit Spectrograph (VIRUS) consists of 156 identical spectrographs (arrayed as 78 pairs, each with a pair of spectrographs) fed by 35,000 fibers, each 1.5 arcsec diameter, at the focus of the upgraded 10 m Hobby-Eberly Telescope (HET). VIRUS has a fixed bandpass of 350-550 nm and resolving power $R \sim 750$. The fibers are grouped into 78 integral field units, each with 448 fibers and 20 m average length. VIRUS is the first example of large-scale replication applied to optical astronomy and is capable of surveying large areas of sky, spectrally. The VIRUS concept offers significant savings of engineering effort and cost when compared to traditional instruments.

The main motivator for VIRUS is to map the evolution of dark energy for the Hobby-Eberly Telescope Dark Energy Experiment (HETDEX[‡]), using 0.8M Lyman-alpha emitting galaxies as tracers. The VIRUS array has been undergoing staged deployment starting in late 2015. Currently, more than half of the array has been populated and the HETDEX survey started in 2017 December. It will provide a powerful new facility instrument for the HET, well suited to the survey niche of the telescope, and will open up large spectroscopic surveys of the emission line universe for the first time. We will

^{*} The Hobby – Eberly Telescope is operated by McDonald Observatory on behalf of the University of Texas at Austin, Pennsylvania State University, Ludwig-Maximilians-Universität München, and Georg-August-Universität, Göttingen

[†] G.J.H.: E-mail: hill@astro.as.utexas.edu

[‡] <http://hetdex.org/>

review the current state of production, lessons learned in sustaining volume production, characterization, deployment, and commissioning of this massive instrument.

Keywords: Telescopes: Hobby-Eberly, Astronomical instrumentation: Spectrographs, Spectrographs: VIRUS, Spectrographs: Integral Field, Spectrographs: performance

1. INTRODUCTION: HET WIDE FIELD UPGRADE AND VIRUS

Large, targeted, spectroscopic surveys of continuum-selected objects are now becoming the norm, and have greatly increased our understanding in many areas of astronomy. Surveys of the emission-line universe, however, are limited currently to wide field imaging with narrow band filters, or to narrower fields with Fabry-Perot etalons or adaptations of imaging spectrographs. Integral field (IF) spectrographs offer a huge gain over these techniques, depending on the application, providing greater sensitivity and wavelength coverage as well as true spectroscopy.

1.1 Large-scale replication of VIRUS

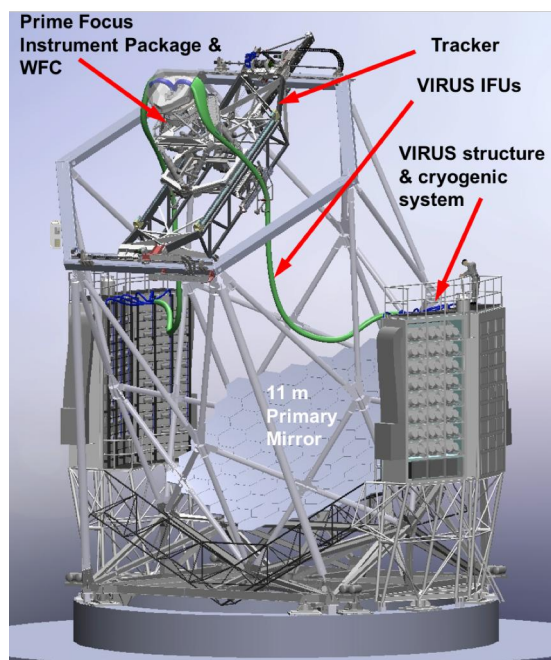


Figure 1 – Upgraded HET. The new tracker supports the Wide Field Corrector (WFC) and Prime Focus Instrument Package (PFIP). The IFU fiber cables run about 20 m to the two enclosures on the VIRUS Support Structure with Cryogenic System that house the 78 pairs of integral field spectrographs that make up VIRUS and the two units of LRS2.

In order to undertake large-scale surveys for emission-line objects, much greater field coverage is needed. Narrow-band imaging surveys can now cover large areas, but often require spectroscopic follow-up, and still do not probe sufficient volume to detect rare objects or to overcome cosmic variance. Wide-field IF spectroscopy requires a large multiplexing factor, so we initiated a program to produce an instrument that uses large-scale replication to create a unique astronomical facility capable of spectroscopic surveys of hundreds of square degrees of sky¹. The instrument is the Visible Integral-field Replicable Unit Spectrograph (VIRUS)¹⁻¹¹, a simple, modular integral field spectrograph that is being replicated 156-fold, to provide an order of magnitude increase in grasp ($\Delta\Omega$) over any existing spectrograph, when mounted on the upgraded Hobby-Eberly Telescope (HET)¹²⁻¹⁷. Fig. 1 shows the upgraded HET as it now appears.

The traditional astronomical instrument has a monolithic design and is a one-off prototype, where a large fraction of the cost is expended on engineering effort. When compared to monolithic instruments, there are cost savings from creating several copies of a spectrograph to gain multiplex advantage, because the components are less expensive and the engineering is amortized over the production run. As an example, the new MUSE¹⁸ instrument for ESO VLT field-slices a 1 arcmin. square field into 24 duplicated IF spectrographs. VIRUS makes the next step, and exploits industrial-scale replication, which we (arbitrarily) define to be in excess of 100 spectrograph channels. We build upon the concepts laid out in Refs. 1-3, where we concluded that industrial-scale replication offers significant cost-advantages when compared to a traditional monolithic spectrograph, particularly in the cost of

the optics and engineering effort. This concept breaks new ground in optical instruments, and appears to be a cost-effective approach to outfitting the coming generation of ELTs, for certain instrument types, where the multiplex advantage of an integral field can avoid growth in the scale of instruments with telescope aperture¹.

The motivation for VIRUS is the Hobby-Eberly Telescope Dark Energy Experiment (HETDEX^{4,8}), which will map the spatial distribution of about 0.8 million Ly α emitting galaxies (LAEs) with redshifts $1.9 < z < 3.5$ over a 420 sq. deg. area (9 Gpc³) in the north Galactic cap and an equatorial field, using VIRUS on the upgraded HET. This dataset will constrain the expansion history of the Universe to 1% and provide significant constraints on the evolution of dark energy.

The advantage of an IF spectrograph for this project is that the tracer galaxies are identified and have their redshifts determined in one observation and the sensitivity is much better than narrow band imaging.

The design of VIRUS flows directly from the requirements for HETDEX, to maximize the number of LAEs detected in a set observing time, and to span sufficient redshift range to survey the required volume. These science requirements flow down to the following technical requirements for VIRUS:

- Coverage of $\Delta z \sim 2$ and coverage into the ultraviolet to detect LAEs at the lowest possible redshift. Analysis of the expected number of LAEs with redshift also indicates that the majority of the objects are located at $z < 3.5$ due to the change in distance modulus with redshift coupled with the steepness of the LAE luminosity function. VIRUS is designed for $350 < \lambda < 550$ nm or $1.9 < z < 3.5$.
- Fiber core size of 1.5 arcsec (266 μ m) for optimal detection of LAEs in the typical image quality delivered by HET (1.3 to 2.0 arcsec FWHM)
- Resolution matching the linewidth of LAEs ($R \sim 700$) to maximize detectability.
- Low read noise detector (~ 3 electrons) to achieve sky-background dominated observations in 360 seconds at the shortest wavelengths
- High stability to ambient temperature variations, though not to gravity variations since the VIRUS modules will be fixed on HET.
- Throughput sufficient to reach sensitivity of 4×10^{-17} erg/cm²/s in 20 minutes on HET.
- Simple, inexpensive design.

Each VIRUS unit is fed by 448 fibers that each cover 1.8 arcsec² on the sky, split between two spectrograph channels. The fibers feeding a two-channel unit are arrayed in a 50×50 arcsec² IFU with a 1/3 fill-factor. A dither pattern of three exposures fills in the area. The spectral resolution is 0.60 nm (resolving power $R \sim 750$ at 450 nm), with coverage of 350–550 nm. The optical design is simple, using three reflective and two refractive elements. With dielectric reflective coatings optimized for the wavelength range, high throughput is obtained. The full VIRUS array will simultaneously observe 35,000 spectra with 14 million resolution elements. In total, VIRUS has 0.7 Gpixels, comparable to the largest imagers yet deployed.

The IFUs are arrayed within the 22' field of the upgraded HET with $\sim 1/4.5$ fill factor, sufficient to detect the required density of LAEs for HETDEX. Development started with the prototype Mitchell Spectrograph (formerly VIRUS-P³), deployed in October 2006, and the production prototype where value engineering was used to reduce the cost for production. VIRUS is now half way through deployment, and we present here results from on-sky commissioning on the upgraded HET.

VIRUS is a joint project of the University of Texas at Austin (UT Austin), Leibniz-Institut für Astrophysik Potsdam (AIP), Texas A&M University (TAMU), Max-Planck-Institut für Extraterrestrische-Physik (MPE), Ludwig-Maximilians-Universität München, Pennsylvania State University, Institut für Astrophysik Göttingen, University of Oxford, Max-Planck-Institut für Astrophysik (MPA), and The University of Tokyo.

1.2 The Hobby-Eberly Telescope and Wide Field Upgrade

The HET¹² is an innovative telescope with an 11 m hexagonal-shaped spherical mirror made of 91 1-m hexagonal segments that sits at a fixed zenith angle of 35°. HET can be moved in azimuth to access about 70% of the sky visible at McDonald Observatory ($\delta = -10.3^\circ$ to $+71.6^\circ$). The pupil sweeps over the primary mirror as the x-y tracker follows objects for between 50 minutes (in the south at $\delta = -10.0^\circ$) and 2.8 hours (in the north at $\delta = +67.2^\circ$). The maximum time on target per night is 5 hours and occurs at $+63^\circ$.

The HET was originally envisioned as a spectroscopic survey telescope, able to efficiently survey objects over wide areas of sky. While the telescope was very successful at observing large samples of objects such as QSOs spread over the sky with surface densities of around one per 10 sq. degrees, the HET design coupled with the very limited field of view of the corrector hampered programs where objects have higher sky densities. In seeking a strong niche for the HET going forward, we initiated a wide field upgrade to increase the field of view to 22 arcmin, coupled with VIRUS in order to exploit the strengths of the telescope and of the site.

The requirement to survey large areas of sky with VIRUS plus the need to acquire wavefront sensing stars to provide full feedback on the tracker position led us to design a new corrector employing meter-scale aspheric mirrors and covering a 22-arcmin diameter field of view. The HET Wide Field Upgrade (WU¹²⁻²³) is now in operation with the wide field

corrector (WFC¹⁹), the new tracker¹⁷, prime focus instrument package (PFIP^{20,21}), and software and metrology systems including wavefront sensing^{16,22}. The WFC has improved image quality and a 10 m pupil diameter. It is designed to feed fibers with a telecentric f/3.65 focal surface. The periphery of the field is used for guiding and wavefront sensing to provide the necessary feedback to keep the telescope aligned as it tracks. The WFC has 30 times larger observing area than the previous HET corrector.

The WFU is commissioned and performing very well, significantly better than the old HET¹⁵. Pointing and tracking are meeting specifications and 4-7 minute setup times are significantly faster than with the old system. The WFC produces excellent image quality over the full field^{15,16,19}. The delivered image size of the HET (1.3-2.0 arcsec., typically) is still dominated by errors of the primary mirror (stack and segment figures) and by dome seeing in cold seasons. Output from the wavefront sensors (WFS) allows image quality to be studied in detail. We are using the several million WFS images obtained in the past two years to study seasonal variations in delivered image quality. For details, refer to Ref. 16.

2. VIRUS PRODUCTION DESIGN

The design, prototyping, and production of VIRUS is described in Refs. 1-11. Here we will provide an overview. The VIRUS instrument consists of three basic sub-units: the IFU, the collimator/grating assembly, and the camera assembly. Each VIRUS unit houses two spectrograph channels (Fig. 2). The motivation for this came first from fiber cable handling: it is more efficient in terms of weight and cross-sectional area to double the number of fibers in a cable (note that the fiber itself is not the dominant weight in a bundle). The volume occupied by the cables is reduced and the cable handling becomes significantly easier with 78 instead of 156 cables to accommodate. The other advantage to the double unit is that two cameras share a vacuum, and have a single connection to the liquid nitrogen (LN) cooling system. This increases the evacuated volume in an individual cryostat, which increases hold-time, and saves cost on vacuum valves and other fixturing. Pairing the spectrographs enabled reduction of mechanical structure to support optics by eliminating the redundant structure of two spectrographs placed side-by-side. The complexity of the enclosures to house the spectrographs was also reduced by pairing the instruments because fewer interfacial features between instrument and superstructure are required.

2.1 Optomechanical design

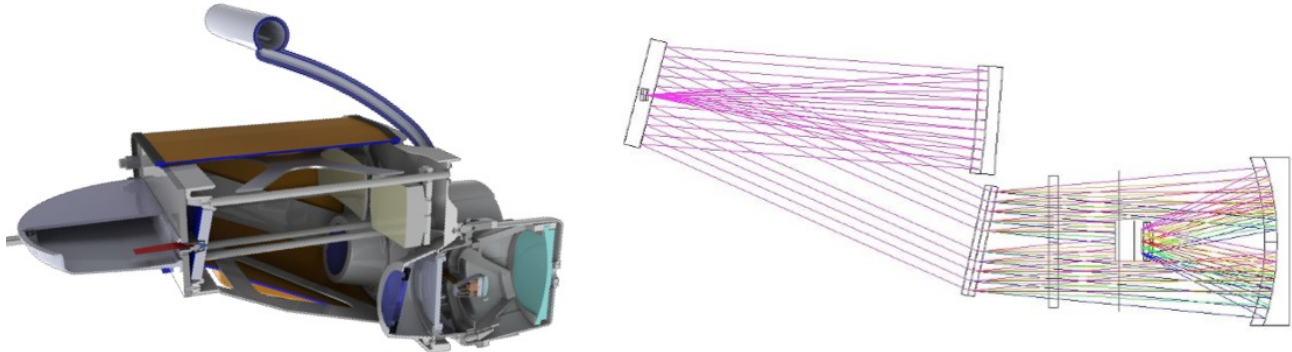


Figure 2: Layout of the production VIRUS. Left shows the production mechanical design and right shows the optical design. The grating has 930 l/mm and the coverage is fixed at 350-550 nm. The mechanical cutaway shows the IFU slit assembly on the left, mounted to the collimator. The f/1.33 Schmidt camera has an internal CCD in the vacuum and mounts to the main bulkhead of the collimator. It is cooled by a flexible line from above with a breakable cryogenic bayonet connection.

The optical layout is shown in Fig. 2. beam size of each channel is 125 mm, allowing the collimator to accept an f/3.32 beam from the fibers, accommodating a small amount of focal ratio degradation of the f/3.65 input from the telescope. The camera is a f/1.33 vacuum Schmidt design with a 2k x 2k format CCD with 15 μm pixels at its internal focus. The three mirrors in the system have dielectric high reflectivity coatings optimized for 350-720 nm. The IFU, collimator, and camera subsystems have kinematic interfaces between them. Cameras are being produced at UT Austin²³, collimators at TAMU²⁴, and IFUs at AIP⁶. Oxford University provided a large number of mechanical parts for the collimators and cameras, and IAG has manufactured many IFU components and the input head mount plate that mounts them to the telescope. Spectrograph integration, alignment, and characterization is led by UT Austin^{5,7,10,25}.

While the VIRUS units are mounted in fixed housings and gravity invariant, their enclosures track ambient temperature and they are required to operate with high stability under a wide range of temperature from -5 to +25 degrees Celsius. The instrument is specified to not require recalibrating for shifts in the positions of the fiber spectra over the temperature range encountered in an hour, with the goal of maintaining alignment during an entire night. Stability is crucial since the data reduction and analysis is sensitive to 0.1 pixel shifts in the spectra. This requirement corresponds to shifts smaller than 0.5 pixels (1/10 of a resolution element) at the detector for 5 degrees Celsius temperature change. This stability was achieved by using an all-aluminum structure with invar-36 metering structures for the collimator mirror focus and the internal structure of the cameras. Angles within the optical path are maintained by the homologous expansion of the structure while flexures accommodate the difference in coefficient of thermal expansion between the aluminum and invar.

VIRUS uses volume phase holographic (VPH) gratings, which offer high efficiency and low cost. Details of the grating design, development, and testing are reported in Refs. 26 & 27. The grating has a fringe frequency of 930 lines/mm and operates at order $m = 1$ in transmission from 350 to 550 nm for unpolarized light. Efficiency is optimized for the UV by lowering the angle of incidence away from the Bragg angle, which is close to 12 degrees. In addition, we specified a 1 deg. tilt of the fringes in the grating, to ensure that the “Litterow” recombination ghost²⁸ is off the detector for the VIRUS configuration.

In order to ensure a standardized reference for measurements of diffraction efficiency of production gratings compared to specifications, and to facilitate rapid testing, we developed a simple rugged grating tester for the specific gratings we are procuring for VIRUS²⁷. LEDs with wavelengths of 350, 450, and 550 nm illuminate a 12.5 mm subaperture on the grating surface. The position of the grating was moved laterally to sample 9 subapertures in order to provide an average efficiency more representative than spot measurements. We have found that VPH gratings exhibit quite significant small-scale variations in efficiency and it is possible to find and report a “hot-spot” in the diffraction efficiency, if too small an area is measured. The grating tester was tailored to the properties we care about in the specification and avoided conflicts over inconsistent measurement methods between vendor and our lab. The contract for 170 gratings was awarded to SyZyGy and production results are reported in Ref. 27.

2.2 Integral field unit cables

For VIRUS we have elected to use a bare fiber bundle to maximize throughput and minimize cost^{6,9,29,30}. The primary advantage of lenslets is in coupling the slower f /ratios of typical foci to the fast ratio required to minimize focal ratio degradation (FRD²⁹), and such IFUs are ideal for retro-fitting existing spectrographs. Lenslets do not provide perfect images, however, so if there is flexibility to choose the input f /ratio to the fibers and if the fill-factor can be tolerated, trading it against total area, the bare bundle provides the best efficiency, as discussed in Ref. 2. Also, the central obstruction of the telescope is preserved at the fiber output to large extent if there is low FRD. This is an advantage for a catadioptric camera as in VIRUS. For the VIRUS IFUs we use a fill factor of 1/3 for the fiber cores, with the fibers in a hexagonal close pack, and dither the IFU arrays through three positions to fill the area.

IFU development at the Leibniz Institute for Astrophysics (AIP)⁶ and University of Texas at Austin (UT)^{29,30} focused on establishing a design that minimizes FRD, maximizes throughput, and is manufacturable in quantity⁶. Careful and rigorous apportioning of tolerances between the components aimed to keep 95% of the transmitted light within the spectrograph pupil (125 mm, $f/3.32$). Figure 3 shows images of the slit and input ends of production fiber cables, along with other views of the IFU assembly. Each IFU contains 448 fibers with 266 μm cores, split between two slits, and we have kept the design as simple and lightweight as possible. The input head consists of a precision micro-drilled block from Euro Micron into which the fibers are fed which is in turn clamped within a stainless steel shell that provides the mounting features. The fibers are glued in with epoxy and then cut off and polished. At the exit, the cable bifurcates within a slit housing into two slits with the fibers glued to grooved blocks. The grooves aim the fibers at the vertex of the spherical collimator mirror. Input and output are bonded to a thin lens and a cylindrical lens, respectively, both of fused silica and AR coated. The lens on the input ensures the chief ray of the curved focal surface is normal to the fiber input for all the fibers, even though the input face is flat.

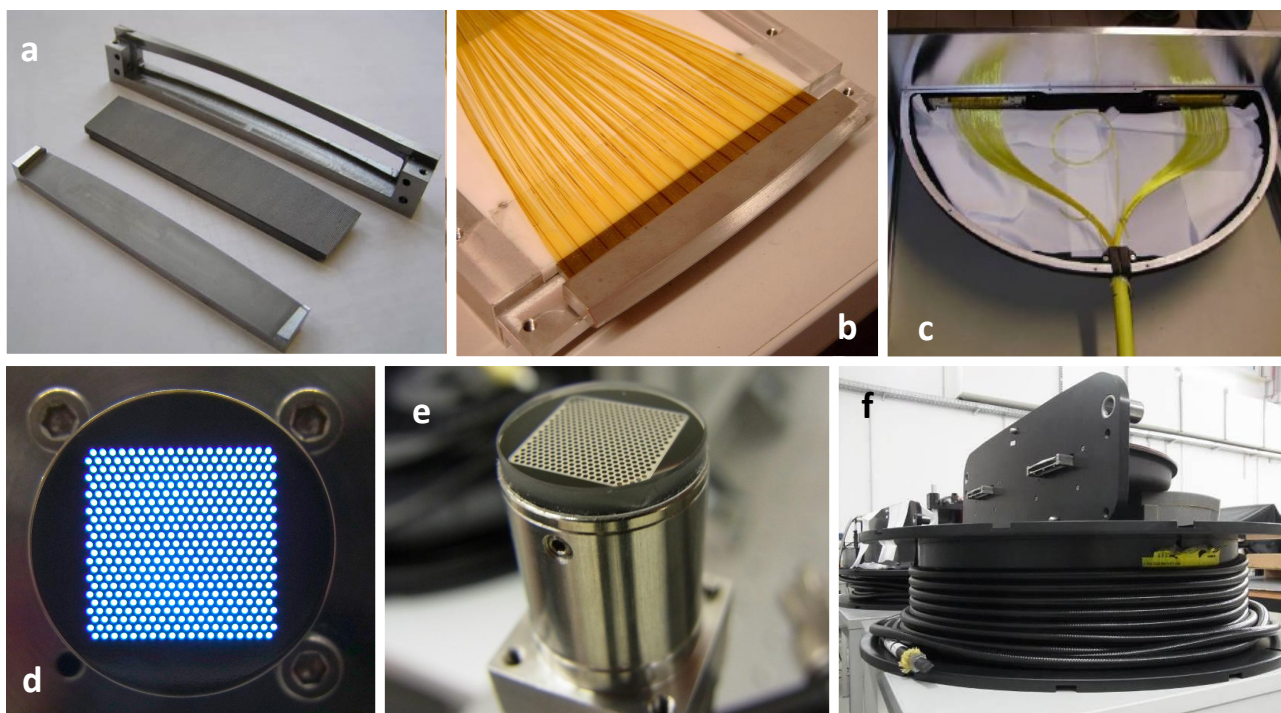


Figure 3. Production of IFU cables at AIP. (a) precision slit assembly components; (b) a slit block with 224 fibers; (c) an integrated output slit assembly with two slit blocks mounted and the fan-out of fibers from the conduit; (d) an input head, back illuminated, with 448 fibers – note the 1/3 fill-factor of the fiber cores; (e) input head with cover lens installed; (f) a completed IFU of 22 m length on transport spool.

The conduit housing the fiber cables underwent extensive design evaluation and prototyping. It is important that the fiber not piston significantly in and out of the conduit where it exits the cable into the slit box. Such pistoning might occur with changes in axial load or ambient temperature swings, and we were particularly concerned about shipping and handling during installation and avoiding twists. We also wished to minimize the weight of the conduit, which can dominate the total weight, and adopted a custom fully interlocked aluminum conduit with PVC sheathing supplied by Hagitec. The ID is 13 mm. As with our previous cables we have an inner sock of Kevlar to protect the fiber from the internal structure of the conduit. The Kevlar sock has a minimum diameter chosen so as not to constrict the fiber, but still fit in the ID of the conduit. The Kevlar is tensioned during assembly, which stabilizes the length of the conduit assembly and prevents fibers “pumping” in and out and developing torsional stress. We took this design through the full range of motions expected at HET in a lifetime test, before production. We simulated 10.2 years of wear (188.7 km of linear travel) on a single fiber bundle. Results of the lifetime test are described in Ref. 30, and qualified the cable design for final manufacture. During the test, we did not see any sign of the fiber pistoning in and out of the conduit at its exit, and this has now been borne out by experience with deployed IFUs at the HET.

In production, we provided the manufacturers with kits of parts (fiber, mechanical parts, conduit, etc.) and they did the assembly and polishing of the ends. Final integration of the slit blocks into the output slit assembly is done at AIP. We established three production lines, based on qualification work at several vendors. One at AIP, and the others at CeramOptec and FiberWare. Acceptance test and evaluation facilities were set up at AIP. These include microscope examination of polish of the input and output ends against fiducial standards, FRD testing, throughput testing, and fiber mapping and position measurement. A final system test is performed on each cable with a fiducial spectrograph unit, generating a report and metadata that are used by the reduction software³¹ and in record keeping.

At the time of writing, all IFUs have been manufactured, and 58 have been characterized and delivered to the HET. Of these, 54 are deployed on sky⁹.

2.3 Camera and Detector System

The camera cryostat vacuum is shared between a pair of spectrographs, reducing part count and increasing evacuated volume. Similarly, the cryogenic cooling system is shared within a unit. This also reduces the part-count of the VIRUS

Cryogenic System (VCS) and reduces losses associated with fittings and valves. The cryogenic system development and testing is described in greater detail in Sec. 4 and Refs. 32,33. The cryostat is composed of two aluminum castings, post-machined only on critical mount surfaces and flanges. Cryostats were manufactured by MKS Inc., following extensive evaluation of prototypes. An impregnating step with Locktite Resinol, following machining, is intended to seal the porosity of the cast aluminum. While the tooling cost for casting is quite significant, the cost for even a single cryostat of this size is competitive with machining from bulk stock, and is much cheaper for the large VIRUS production run. We have subsequently discovered that we need to carefully leak-check the cryostats using a residual gas analyzer in order to find and fix small leaks that compromise the hold time. Applying epoxy to the leak locations results in consistent vacuum performance.

The CCDs for VIRUS have a nominal 2kx2k format with 15 μm pixels. The required readout time is relatively slow at 20 seconds, binned 2x1, but low read noise (~ 3 electrons) is required and the parallel readout of 156 CCDs distributed through the volume of the HET structure is challenging. The VIRUS system is 665 Mpixel, which is comparable to MUSE³⁴ and to the largest imaging mosaics yet deployed. The data volume from the full VIRUS array is about 2.5 GB per observation. The integrated detector system was supplied by Astronomical Research Cameras, Inc. (ARC), with the University of Arizona Imaging Technology Laboratory (ITL) providing thinned backside illuminated CCDs with AR coatings optimized for the VIRUS bandpass, as a subcontract from wafers manufactured by Semiconductor Technology Associates, Inc (STA). Since the CCDs come from custom wafer runs, we elected to increase the imaging area to 2064 by 2064 pixels, allowing more latitude for alignment. The device is designated STA3600.

The design of the detector package, flex circuit, and controller were customized to the VIRUS application, since the engineering effort is spread over a large production run. Figure 4 shows the assembly of a pair of detectors in a cryostat. The CCD package, machined from Invar-36, is designed for minimum obstruction and hides in the shadow of the field flattener (FF) lens. The CCDs are flat to within $\pm 10 \mu\text{m}$, which is allowed by the tolerance analysis. The package has a custom header board that brings the traces to a single connector on one side of the package. A custom flex circuit with complex geometry connects the two detectors to a single 55-pin hermetic bulkhead connector. The controller mounts directly to this connector, without cables, and its form-factor was customized to fit between the cylinders of the cryostat cover.

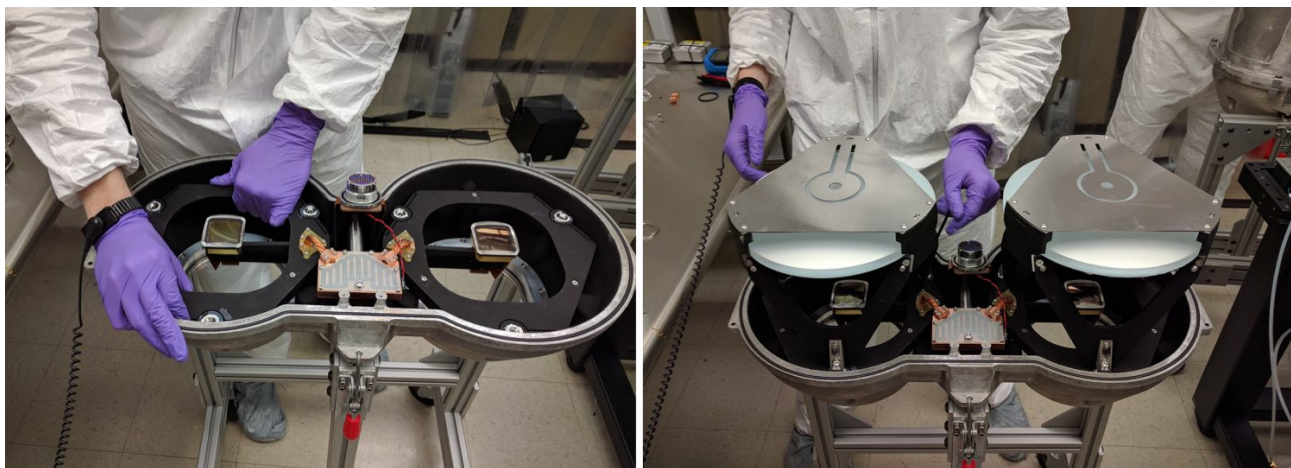


Figure 4: Assembling a VIRUS camera. Left shows two CCDs with integrated field flattener lenses mounted on cast invar “spiders” with cold links and flex circuit, integrated in the cast aluminum camera body. Right shows the two camera mirror assemblies integrated, prior to installation of the camera cover, also of cast aluminum. All parts of the CMAs are invar. The flexures at the top are bonded to bosses at the centers of the mirrors, with mirror adjustments at the three corners that are accessed via vacuum feed-throughs on the adjuster back, during alignment.

The CCD and FF alignment tolerances are the tightest in the system. Initially we aligned and bonded the FF in-situ³¹, but this caused some deposition of epoxy in the corners of the CCDs during cure due to outgassing. We modified the procedure to provide separate alignment references for FF and CCD that allow the FF to be bonded to its mount separately from the CCD. Two alignment stations incorporating alignment telescopes allow a CCD and FF to be bonded simultaneously¹⁰. The CCD is mounted in the cast invar “spider” which has a minimum-obstruction arm to suspend the

detector in the beam. The CCD is aligned in a second alignment fixture by adjusting the three spider mount points which are then glued to set the alignment. After 24 hours cure time, the FF lens is installed onto the detector package.

Two spider assemblies are integrated with cold links and flex circuit and then mounted in the camera body (Fig 4, left). The three mount points of each spider interface with precise features post-machined into the aluminum casting. In this way, the alignment of the CCD and FF to the axis of the camera is achieved within the required tolerances of 50 μm in centration and separation, and 0.05 degrees in tilt¹⁰. Since the camera mirror assembly mounts to the same points, the entire camera becomes a unit with only the aspheric corrector plate (with much lower alignment tolerances) separate (Fig 4, right).

The CCD controllers have DC power in and fiber-optic data lines out. In the ARC system, the data system requires several levels of multiplexing. First, each CCD controller commands two detectors, each with two readout amplifiers. Next, a custom-built 8-way multiplexer combines the output from each set of 8 CCD controllers. Next, the output of each of 12 multiplexers is fed into a separate PCI interface card. Two PCI-to-PCIe expansion chassis are used to connect 6 PCI interface cards each to a PCIe port in the VDAS computer. Finally, the data are transferred via DMA from the PCI interface cards into the VIRUS data computer memory. This architecture has proven unstable as we have added units to the array. Modifications to the architecture have improved the situation and others are being studied. This work will be reported elsewhere. Readout is controlled by the CAMRA control system written in C++ and integrated within the HET Telescope Control System (TCS)²².

As reported in Ref. 7, the original detectors for VIRUS suffered from failures triggered by contamination that caused significant QE depressions as well as small clusters of low-QE pixels, particularly at the corners. We were able to identify detectors with sufficiently good cosmetics to deploy 16 units to advance the understanding of the system and start commissioning the instrument. In the meantime we have procured a new wafer run from STA and ITL has been processing them along with wafers left over from the original procurement. These “generation 2” detectors have a thicker epitaxial layer along with processing changes that produce excellent results. At the time of writing, more than 50 new CCDs have been delivered. 26 units with these “gen 2” CCDs are delivered to HET. 14 units with the original CCDs remain in the array.

3. VIRUS ALIGNMENT AND CHARACTERIZATION

Following assembly of collimators and cameras, the spectrographs are integrated and aligned. The alignment procedure involves attaching an adjustment back to the camera cryostat, in place of the regular back, that incorporates ferrofluidic vacuum feed-throughs for adjustment and locking of the camera mirrors. We also allow small adjustments of the collimator position. Experience with aligning VIRUS-P highlighted the likely bottle-neck of this step in the large-scale production and led us to develop a deterministic alignment procedure that utilizes moment-based wavefront sensing (MWFS) analysis^{10,35,36}. This MWFS method relies on the geometric relation between the image shape moments and the geometric wavefront modal coefficients. The MWFS method allows a non-iterative determination of the modal coefficients from focus-modulated images at arbitrary spatial resolutions. The determination of image moments is a direct extension of routine centroid and image size calculation, making its implementation easy in the alignment of real systems like VIRUS. The alignment procedure can be accomplished in 3 hours per channel, once the detectors are cold, and is described in detail in Refs. 10, 35 & 36. The resultant image quality exceeds the specifications in most cases, due to the exceedingly good FF to CCD alignment that is achieved.

Following alignment, VIRUS units undergo a characterization^{37,38} before being packed for transport to the HET. The characterization station is located in a separate lab that can be darkened sufficiently to ensure no stray light for the tests. A lab calibration unit houses a laser driven light source (LDLS, see below) for flat-fielding and Hg+Cd line lamps for wavelength determination. A standard production IFU is designated for these tests so there is a uniform reference. In addition, a “pixelflat” head that mounts in place of the IFU head and provides a continuous illumination of the two slits rather than the highly modulated IFU output is utilized to provide the source for pixel-flat-fields of the detector, free of the spatial dimension fiber modulation. This is important for generating maps of the pixel-to-pixel QE variations and to identify bad pixels. A third IFU has a mask to sparsely-select fibers for characterization of scattered light and profile shapes. Bias levels are set and photon transfer curves are generated to confirm read noise and gain of each channel. Sets of bias and dark frames are recorded to act as a reference once the units are installed at HET. Python scripts provide automated characterization datasets and reports in conjunction with the CAMRA readout system.

Figure 5 shows some examples of outputs from characterization of VIRUS spectrographs and IFUs. The spectrographs produce excellent image quality and the fiber profiles are characterized using the sparsely illuminated IFU input. The profiles are well fit by a Gaussian-hermite function with exponential wings. The wings contain about 3% of the light in the core and are consistent with the scattering expected from the surface roughness specifications of the spectrograph optics. Fig. 5 also shows the excellent separation (contrast) between fibers that is achieved in the alignment process^{35,36}. The lower panels in Fig. 5 present two examples of the IFU fiber-to-fiber throughput measured relative to the highest throughput fiber. Typical variations are around 10% peak to peak, with some systematics depending on the fiber location in the slits.

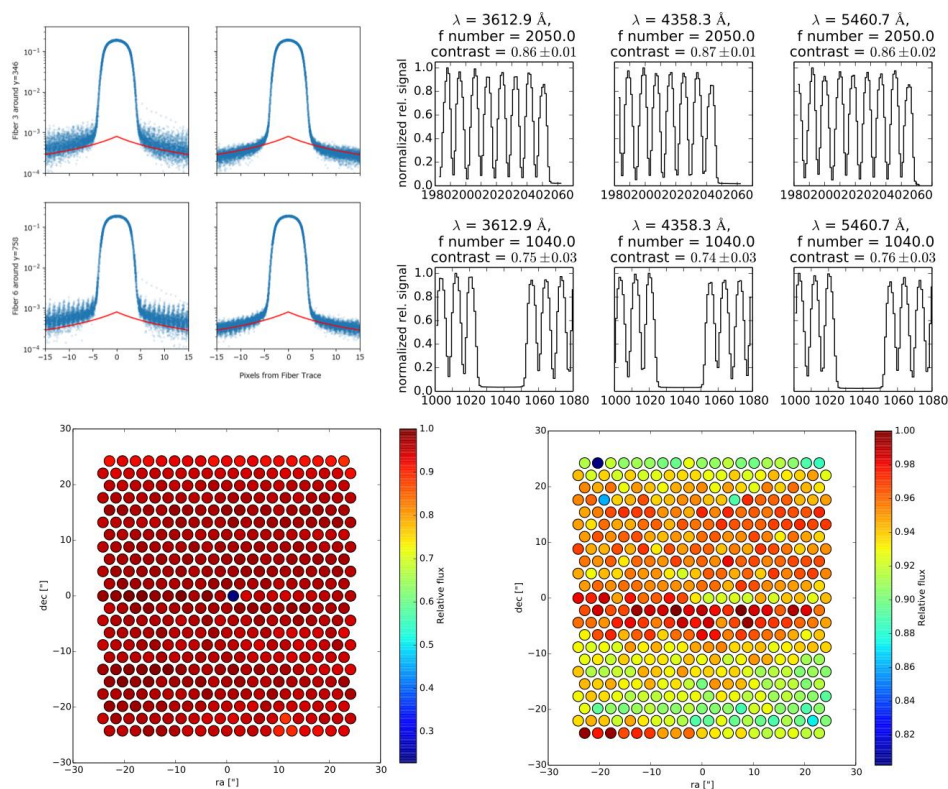


Figure 5. Examples of characterization data obtained on VIRUS spectrograph units and IFUs. Top left, fiber profiles in the spatial dimension measured as part of the spectrograph characterization, plotted on a logarithmic scale, showing Gaussian-hermite core and exponential wings, in red. The wings sum to ~3% of the integrated core flux and account for all the light between fibers. Top right, fiber profiles measured as part of the IFU characterization showing 6 places on the detector and indicating very good contrast numbers between the peak and trough of the profiles. The lower two panels show examples of fiber throughput relative to the peak fiber for two IFUs. The axes are nominal fiber position from the center expressed in arcseconds projected on sky. The split between spectrograph channels is at the center of the IFU and horizontal. Typical non-uniformity is at the 10% level.

4. VIRUS INFRASTRUCTURE ON HET

VIRUS and LRS2 are fiber-fed which allows the mass of the spectrographs to be carried in two enclosures, one on each side of the telescope (Figs. 1,6). Each enclosure³⁹ can support 40 pairs of spectrographs, there is capacity for the 78 VIRUS units and the two units of LRS2. The VIRUS support infrastructure, installation, and maintenance procedures are described in Ref. 11. The final VIRUS enclosure locations were a compromise that was strongly influenced by the need to maintain man-lift access to the primary mirror. Since the wavelength coverage of VIRUS extends down to 350 nm, the average fiber length had to be minimized commensurate with keeping the mass of the instrument off the telescope structure and providing sufficient access to the primary mirror and tracker with the HET man-lifts and crane. Following extensive optimization and evaluation by HET staff, we settled on a configuration with VIRUS units housed in two large enclosures flanking the telescope structure and riding on a separate air-bearing system during rotation of the telescope in azimuth (Fig. 1). The VIRUS Support Structure (VSS) is a complex weldment that interleaves with the main telescope structure

without applying loads to it that could couple wind induced vibration from the enclosures to the telescope. It rides on separate air-bearings that lift it during changes in telescope azimuth, and is pulled round by the main azimuth drive. The enclosures are large clean rooms with air circulation and heat extraction to remove heat from the VIRUS controllers and ensure that the skin temperature of the enclosures remains close to ambient to ensure they do not impact the dome seeing. The weldments for the enclosures were procured by MDO and were outfitted with hatches, seals, cables and the heat removal system by TAMU³⁹.

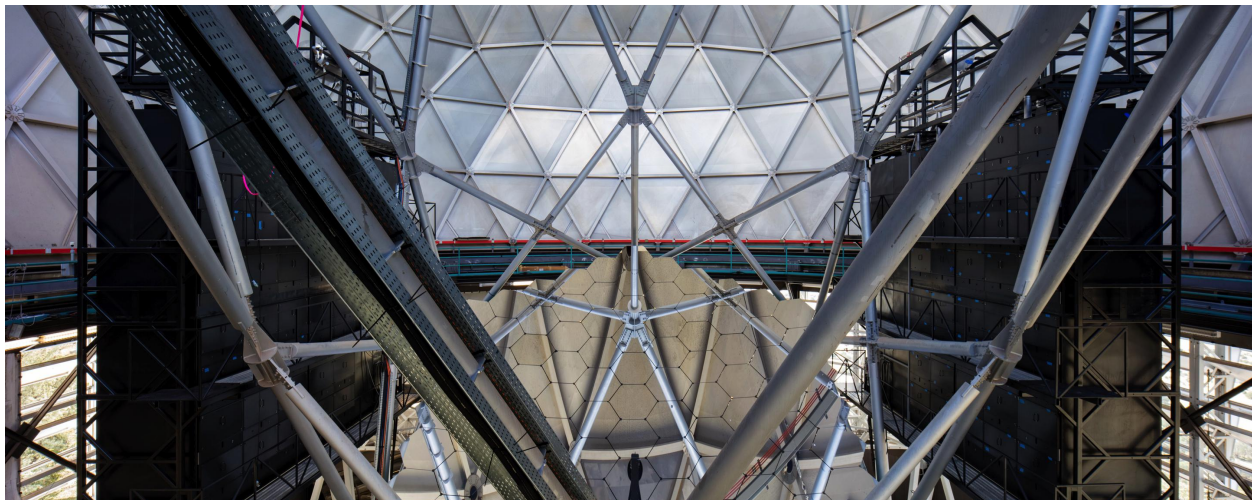


Figure 6: View of the HET from the front showing the primary mirror and the large VIRUS enclosures either side of the telescope structure. They sit on the VIRUS support structure (VSS), which moves on air bearings to follow the azimuth setting of the telescope. The phase separator tanks of the VIRUS Cryogenic System (VCS) can be seen mounted to the top of each enclosure.

The distributed and large-scale layout of the VIRUS array presented a significant challenge for the cryogenic design^{32,33}. Allowing 5 W heat load for each detector, with all losses accounted for and a 50% margin, the cooling source is required to deliver 3,600W of cooling power. We engaged George Mulholland of Applied Cryogenics Technology to evaluate the options and provide an initial design. Following a trade-off between cryocoolers, small pulse-tubes and liquid nitrogen based systems, it was clear that from a reliability and cost point of view liquid nitrogen is the best choice³². The problem of distributing the coolant to the distributed suite of spectrographs is overcome with a gravity siphon system fed by a large external LN tank. A trade-off between in-situ generation of the LN in an on-site liquefaction plant, and delivery by tanker has been made, with the result that the delivery option is both cheaper and more reliable.

An important aspect of the cryogenic design is the requirement to be able to remove a camera cryostat from the system for service, without impacting the other units. This is particularly difficult in a liquid distribution system. A design was developed that combines a standard flexible stainless steel vacuum jacketed line (SuperFlex) to a cryogenic bayonet incorporating copper thermal connector contacts into each side of the bayonet. When the bayonet halves are brought together they close the thermal contact. The resulting system is completely closed, i.e., it is externally dry with no liquid nitrogen exposure. The camera end of the connector is connected by a copper cold finger to the detector. This design has another desirable feature: in normal operation the SuperFlex tube slopes downwards and the bayonet is oriented vertically. Liquid evaporation will flow monotonically up in order to avoid a vapor lock. If the bayonet is unscrewed and raised upwards, a vapor lock will occur and the bayonet will be cut off from the cooling capacity of the liquid nitrogen. This effectively acts as a “gravity switch”, which passively turns off cooling to that camera position.

The VIRUS Cryogenic System (VCS) was constructed by Midwest Cryogenics⁵. The 11,000 gallon vacuum jacketed tank was installed by Praxair in October 2014. The enclosures were delivered to HET and the VCS installed in Nov 2014 and Feb 2015. The system was first turned on in Feb 2015 and now operates continuously, cooling more than 40 spectrograph units distributed in both enclosures. A 6,000 gallon delivery of LN is required every two to three weeks. Praxair is making regular deliveries triggered by metrology on the main tank that indicates LN level.

An essential part of VCS is its safety system. This system continuously monitors critical variables (e.g. dome atmosphere oxygen levels, LN pressure, LN flow rates, and LN storage tank levels). When predefined set points are exceeded the system automatically activates strategically located audio and visual alarms, and if required closes the main

LN supply line valve. Each afternoon the system undertakes an auto-test of the alert system, and sends test telephone alerts to the recipient list. This ensures that the system cannot go off-line for an extended period without being noticed.

5. VIRUS DEPLOYMENT AND PERFORMANCE

The first 16 VIRUS units were deployed in May 2016^{7,40} and at the time of writing we have deployed 40 VIRUS units and 54 IFUs on HET, along with the two units of the new low-resolution spectrograph (LRS2-B and LRS2-R⁴¹) that also utilize the VIRUS cryogenic, enclosure, and readout infrastructure. Installation of spectrograph units is described in Refs. 11 & 40 and installation of the IFUs is described in Ref. 9. The HET staff are routinely installing and maintaining VIRUS units as described in Ref. 11. Figure 7 shows images that illustrate aspects of the installation.



Figure 7: VIRUS spectrograph unit deployment; (a) 8 units staged for installation in HET receiving bay; (b) VIRUS unit rigged and balanced for lifting with HET dome crane; (c) 8 units installed in one of the VIRUS enclosures, prior to installation of enclosure covers; (d) IFUs installed on the other side of the enclosures, or awaiting installation after stringing from the tracker.

5.1 Hardware deployment

Deployment of the IFUs happens in batches and precedes spectrograph installation, which happens typically in deliveries of 1-3 units. Careful planning has resulted in quite rapid deployment of IFUs, but the telescope is off line for several nights during the process since the input head mount plate (IHMP) assembly is removed to a work platform on the tracker and we disable motions of the tracker during the deployment⁹. We can deploy typically 8 IFUs per day and currently have 54 mounted (Figure 8).

Before mounting on the spectrograph unit, each IFU is inspected for any stress that might have been created in the tailpiece, by removing the inspection cover to look at the fibers going to the slit blocks (Fig. 3,c). Adjustments can be made to the conduit clamp in the tailpiece, if needed (which is rare). The tailpiece is then mounted to the kinematic mounts on the spectrograph unit and the enclosure sealed up. IFU tailpieces are inspected periodically to look for evidence that the fibers are becoming taught due to axial motion within the conduit over time. We do not see any evidence that such motions are taking place, so the IFU system is robust in the deployment at HET.

Figure 8 shows the front view of the deployed IFU input heads for VIRUS and LRS2, and the input to the fiber feed for the Habitable-zone Planet Finder⁴², near infrared high resolution spectrograph developed by Penn State University.

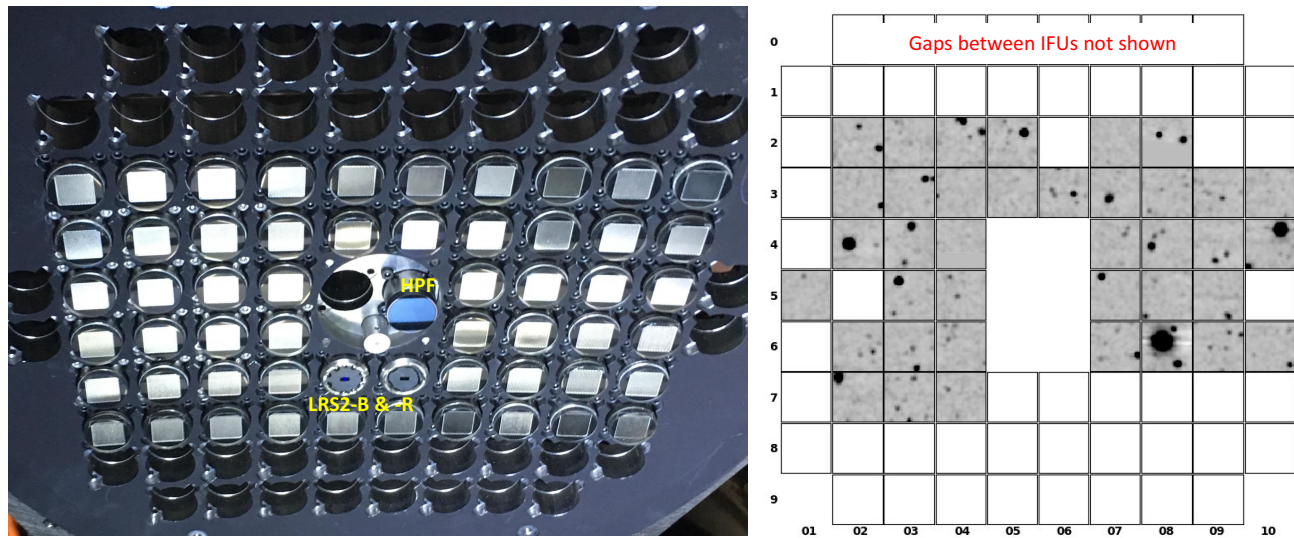


Figure 8: Left – photon’s-eye view of the deployed IFUs for LRS2 and VIRUS mounted in the precision input head mount plate (IHMP), along with the fiber feed for the HPF high resolution spectrograph. LRS2 has two small full-fill IFUs mounted close to the central mounting boss for the high resolution spectrographs, where the fiber feed for HPF is mounted. The other central hole is for the future HRS2 high resolution spectrograph. The LRS2-B and LRS2-R IFUs are 100 arcsec. apart on the sky, which is the same pitch as for the VIRUS IFUs. 54 VIRUS IFUs are installed, currently. Each covers 50x50 sq. arcsec. For scale, the corner VIRUS IFUs in this image are ~18 arcminutes apart, which is ~190 mm. Right – example of data from VIRUS on a typical HETDEX field with 39 spectrograph units deployed. The spectral dimension is collapsed to create images for each IFU, and this representation does not show the gaps between the IFUs.

5.2 Instrument and system commissioning

Upon delivery, the basic behavior of the VIRUS units is established using the Facility Calibration Unit (FCU), which injects flat field and emission-line source light into the entrance of the WFC and mimics the ray bundles propagating through the optical system. For VIRUS we use a Laser Driven Light Source with a laser pumped Xenon plasma (LDLS[§]) for flat fielding to provide adequate UV light along with Hg and Cd emission line lamps. While each IFU plus spectrograph unit has not been tested together as a pair before, we find a good correlation between performance in lab and on the telescope, indicating that we can align the IFUs and spectrographs separately against fiducial units and achieve our requirements when they are combined finally at the telescope.

In operations, Python scripting of the TCS/CAMRA system allows various combinations of calibration data to be taken utilizing the FCU. Scripts are run each night to obtain standard sets of calibration data (flats, arc lamps, bias, darks), along with twilight flats that provide the baseline calibration. A short version is used each afternoon to check the health of the system during the operations checkout period between the day and night staff shifts.

Monitoring the state of VIRUS over time requires a significant level of automation and digestion of metrics. It is much more complicated than for an imaging array of similar pixel count. The VIRUS Health Check (VHC) script runs on all data as it is obtained. VHC is based on the Cure data reduction package³¹, and catches data problems and provides a graphical interface for the Resident Astronomers to monitor the system. This is especially helpful during afternoon operations checkout where test calibration data is taken with the FCU to ensure any problems with the system are caught before science operations start. The scale of VIRUS means that such automation is essential to catch problems in a timely manner. Bias levels, flat field levels, noise, and missing bits are checked, among other tests.

VHC gives an instantaneous check of the data and can flag units that are off-line, but still reading out, due to vacuum maintenance or other reasons. Long-term monitoring of properties such as bias level, read noise, dark count, fiber throughput, channel throughput, image quality and image position is needed to flag changes that might impact the science

[§] Model EQ-99X-FC-S from Energetiq

data product. Systems for this monitoring are still being developed. With half the array populated, it is very clear how crucial they will be.

The physical stability of the spectrograph channels is excellent, as monitored by shifts in the position of the spectra on the detectors. Typical shifts of the spectra are 0.1 pixels per 5 C, which is about a factor of five better than the requirement. For reference, a resolution element is ~ 5 pixels, so shifts are 0.4% of the image size per degree C. The quality of sky subtraction is sensitive to shifts at the 1% level, due to the very strong modulation of the spatial profiles due to the fibers. So, in retrospect, we would specify stability more stringently than 0.1 pixels/degree C, and require it to be in line with what we are achieving with VIRUS.

Flux calibration of the data involves correction for the normalization of the 3 individual dithered exposures that make up an observation, using photometry from the guidestars. Their normalization changes with tracker position and observing conditions. Dithering is made with guider fiducial offsets. Spectrophotometric standard stars are observed on one IFU each night. The flux calibration is also obtained from ~ 10 stars that fall on the IFUs in a typical observation, by referencing to SDSS photometry. The calibration between IFUs is made by referencing to twilight sky observations and assuming they are flat over the field of view of VIRUS, ~ 0.3 deg. diameter. Calibration to 8% at any wavelength is routine and we are working to achieve 5%.

Observations of globular clusters proved to be particularly important in commissioning. Hundreds of stars allow the IFU positions to be measured accurately, and also demonstrate that the image quality of the HET is uniform over the field of view. Since the VIRUS units provide the only measurements over the full science field of the upgraded HET, these observations have also proven important in verifying HET performance, particularly image quality. Detailed wavefront measurements over the science field were obtained with small deployable wavefront sensors that mounted in the same seats as the IFUs and hence tie together the physical and optical focal surfaces of the telescope. These measurements vindicated the alignment of the WFC and showed that the optics system meets image quality specifications. See Ref. 16 for details of this process. VIRUS observations have helped to confirm that the image quality is almost independent of field angle, at least down to about 1.5 arcsec FWHM, and tie together images obtained with the acquisition camera and the guide probes.

We have been able to measure the differential atmospheric refraction (DAR) with high precision from GC data, and can fit the shifts with a simple model. We chose not to have an atmospheric dispersion compensator for VIRUS because even a complicated optic would have residuals from the compensation that would be difficult to model. We can easily model the DAR in the VIRUS data from the data themselves and a simple model, so we can correct positions to a fiducial wavelength of 550 nm. This is a particular advantage of IFU instruments, which can follow the DAR and gather all the light independent of wavelength.

A few IFUs have exhibited fringing when deployed. This is traced to poor bonding of the cylindrical lenses on the exit slits of the IFUs, and in particular to the use of Norland UV curing adhesive for this bond, early in production. Small bubbles would result which cause few percent fringing modulation of the throughput of the system with wavelength. The majority of the IFUs use a coupling gel rather than the UV curing adhesive, and do not show this feature. Five IFUs exhibiting fringing have been identified and repaired or are scheduled to be removed from the array for repair in Austin.

5.3 Throughput and sensitivity

The throughput of the system of VIRUS units and the HET was predicted during the PDR phase of HETDEX², and sensitivities and number of detected emission line objects were derived and compared to science requirements. Typical observing conditions were included so that predictions were realistic. From this analysis, we established the required number of fibers and hence the number of VIRUS units needed. We also flowed the overall throughput down to the individual component level in order to establish requirements for the minimum performance of each component along with mean performance requirements for batches of components. In this way we could allow manufacturers some leeway for the inevitable range of performance without having to reject many components with the resulting increase in cost. The components that most effect performance are the IFU, grating, and CCD. The reflectivity specifications for the multi-layer dielectric reflectors were sufficiently stringent that they do not contribute much to the dispersion in properties.

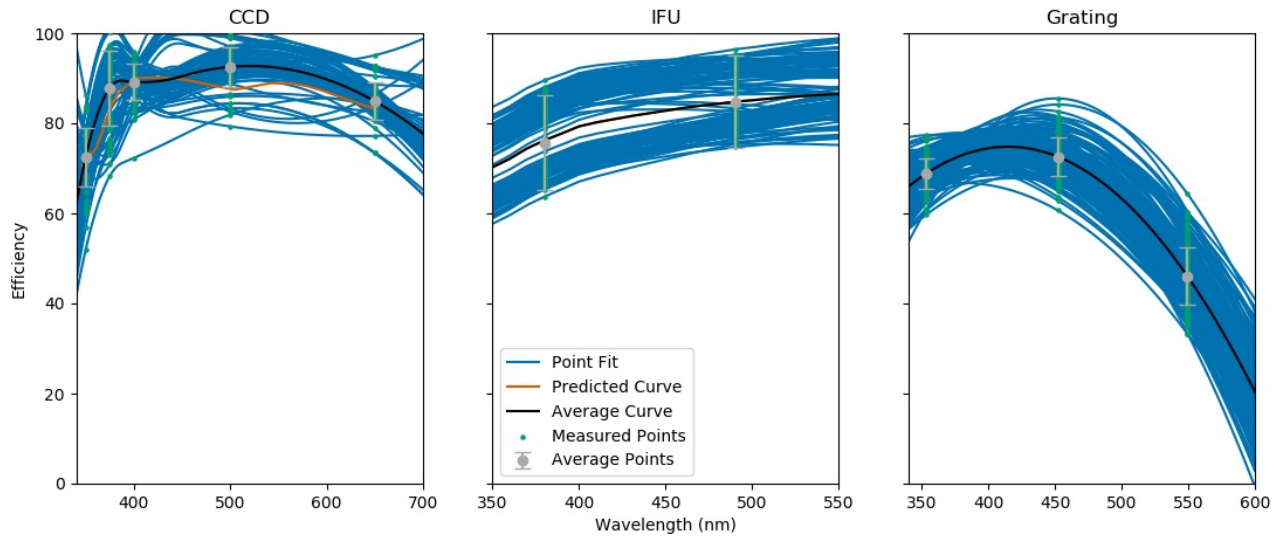


Figure 9: Efficiencies of individual components of VIRUS. Left is the CCDs, middle the IFU fibers, and right the gratings. Data points are shown in gray along with means and standard deviation. Fits to interpolate the data points are shown in blue. For the CCDs a cubic spline is used, fit to the 5 data points. For the IFUs, the typical throughput shape is fit to relative throughput measurements at two wavelengths by multiplying by a first-order polynomial. For the gratings, cubic splines were fit to three measured wavelengths. See text for details.

The VIRUS units incorporate 156 spectral channels which are individual realizations of the same spectrograph with the varying performance of the individual components. In Ref. 38 we discuss the range in properties of the VIRUS components and construct multiple realizations of the spectrograph to explore the expected range of properties. This is an extension of work first reported in Ref 37. Fig. 9 presents the range of efficiencies for the CCDs, IFUs, and gratings. The CCDs have quantum efficiencies reported by ITL at 5 wavelengths spanning 350 to 550 nm. In order to interpolate between those wavelengths, we fitted cubic splines to the data points. As shown in Fig. 9, the spline values occasionally exceed 100% but mostly create a representative interpolation and in the average agree quite closely with a typical efficiency curve measured by ITL for similar CCDs on a finer wavelength grid. The IFUs were assembled and tested at AIP. Each fiber bundle was delivered with a report, assessing its performance overall and on a fiber-to-fiber basis (examples are shown in Fig. 5). These reports present measurements of the relative throughput of each fiber bundle at two wavelengths. Photodiodes with narrow band filters are used to normalize variations in the light input across IFUs. The interpolated curve is obtained by multiplying a typical throughput curve by a first-order polynomial to tilt it such that it passes through the measured points. For the gratings, we supplied SyZyGy with a tester that measured the throughput at three wavelengths²⁷. These datapoints were fit with a cubic spline, which we had previously shown to be a good approximation to the efficiency curves of model gratings²⁷. Further information and data on the reflectivities of the three mirrors can be found in Ref. 38.

Figure 10 presents the results of combining the component efficiencies into 156 random realizations of the spectrograph channel throughput along with the average. The spread is approximately $\pm 20\%$ at all wavelengths, which is in line with expectations for the specifications of the components. Fig. 10 also compares the average to the model of VIRUS throughput discussed above. The model and this derived throughput both include a field and wavelength dependent correction to account for the obstruction of the detector package in the Schmidt camera of VIRUS. For perfect FRD the central obstruction of the telescope is preserved in the pupil illumination within the spectrograph, so at the center field the obstruction removes less light than at the edges of the field. The primary effect of FRD is to scatter light into the central obstruction since modes at larger f-number are more numerous. As a result, poorer FRD performance would result in less variation of throughput with field angle within the spectrograph. The model assumes perfect FRD and varies by 7% from center to edge of field (wavelength). Tests of FRD of fibers in VIRUS IFUs indicates very good performance³⁰, so this assumption is likely to be valid. The ends of the wavelength range presented the greatest challenge for meeting throughput requirements, due to the fiber transmission, CCD QE and grating blaze in the UV and the grating blaze at the green end of the spectrum. This fact is reflected in the higher throughput performance than required in the middle of the wavelength range and the slight shortfall at the extreme ends. Overall, this comparison indicates that the predictions of component

performance were realistic and the specifications supplied to the manufacturers could be met or exceeded over most of the bandpass on average.

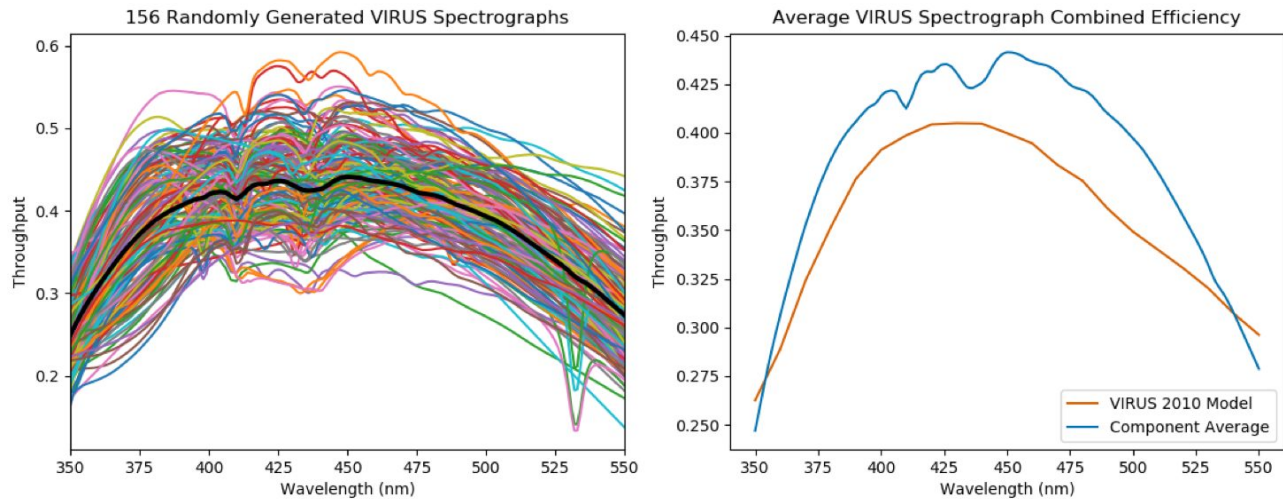


Figure 10. Predicted VIRUS unit throughputs without the telescope. Left presents 156 realizations of the spectrograph channel throughput made by multiplying randomly selected real components, along with a model for the spectrograph obstruction. The black line is the mean of the 156 channels. Right shows the same average curve compared to the prediction from 2010 on which the VIRUS specifications were based. That prediction incorporates the same obstruction model, so the higher throughput in the middle of the wavelength range reflects the component performance being better than specifications except at the extreme ends of the wavelength coverage.

A comparison can be made between these predictions and the measured on-sky performance by combining them with a model of the HET. The HET model includes the WFC obstructions and primary mirror illumination with the tracker on axis, and accounts for those losses relative to a 10 m unobstructed aperture above the atmosphere with an atmospheric extinction model at $AM=1.25$, the mean for HET over a track. The HET model includes the measured WFC coatings and also includes an estimate of the degradation of the bare aluminum reflective coatings on the HET primary mirror for an average segment age of 12 months. Degradation rates were estimated from data taken on bright stars with the segments tilted out of alignment to produce separate images, and reflectivity compared to freshly coated segments. For example, at 370 nm a degradation rate of 2% per month is estimated.

The measured VIRUS throughput was bootstrapped from detailed measurements with LRS2. Spectrophotometric standards are observed every night with LRS2 and the most pristine conditions are selected to measure the throughput of the system for 370-1050 nm. The small full-fill factor IFUs of LRS2 allow all the photons from a star point-spread-function (PSF) to be counted. It is harder to account for a star's PSF with VIRUS due to having to take three dithered exposures to fill in the fiber pattern. The VIRUS throughput curve was obtained by comparing simultaneous observations of the sky between LRS2-B and VIRUS, accounting for the different spatial element scales and the field illumination pattern of the HET. The VIRUS throughput is the average of 80 deployed channels corrected to center field, center track. Fig. 11 shows good agreement in the shape of the system response, but a small shortfall $\sim 7\%$ compared to expectations. This shortfall could easily be due to an inaccuracy in the model of the HET reflectivities or some FRD scattering light into the central obstruction at the pupil of the spectrograph channels. However, the good agreement in the shape of the system response suggests that the optics obstruction model assuming good FRD performance is probably valid.

Fig. 11 also shows the variation in on-sky throughput for the 80 spectrograph channels, corrected for the HET field illumination pattern. The curves are generated from twilight sky observations to produce normalized relative throughput for each channel compared to the average. These normalized curves are then multiplied by the average throughput. There are two channels with low throughput that are associated with a malfunctioning readout in one unit. Overall, the performance of the spectrograph channels is in good agreement with expectations. We worked hard to preserve as much throughput at 350 nm as possible, in spite of the combined challenges posed by fiber length, CCD efficiency and atmospheric transmission, since the majority of LAEs will be detected between 350 and 450 nm due to their distance modulus and luminosity function. Another way to evaluate the performance is to compare detection sensitivities with predictions. The noise in blank sky spectra is extremely well characterized since most fibers are looking at sky most of the

time. The 5-sigma noise per resolution element measured from the sky data indicates a line flux detection threshold of $4.0 \times 10^{-17} \text{ erg/cm}^2/\text{s}$, at 450 nm, which agrees well with the predictions.

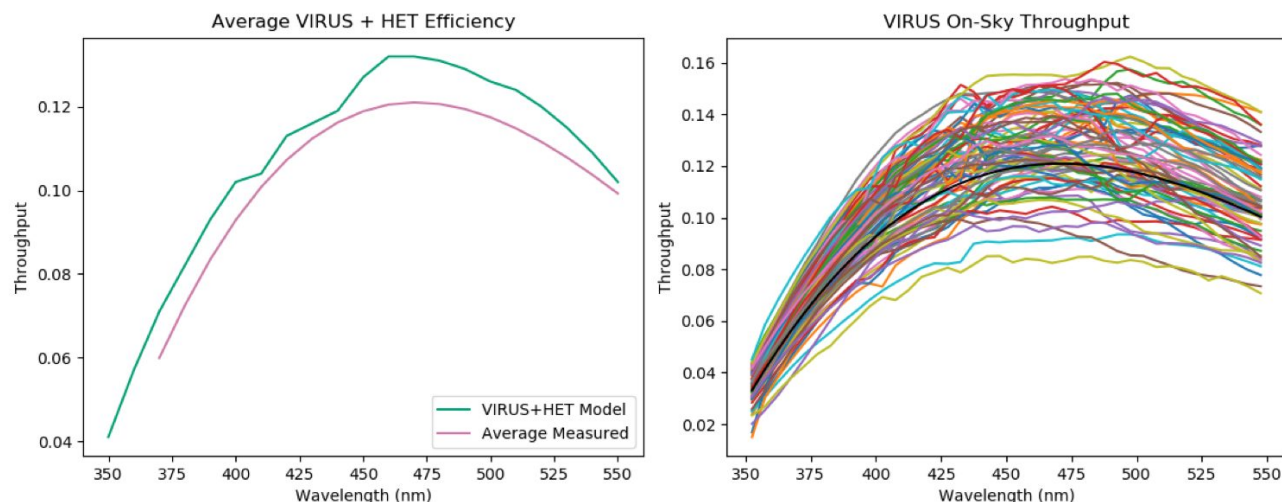


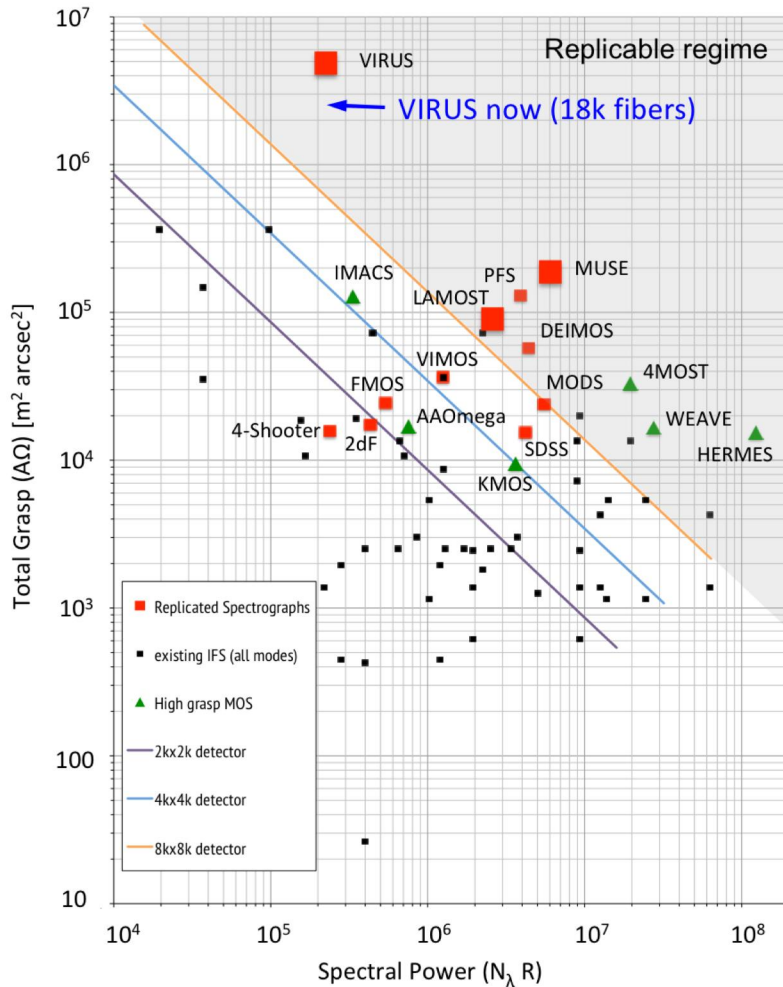
Figure 11. On-sky throughput of VIRUS plus HET and atmosphere, compared to expectations. Throughput is relative to an unobstructed 10 m aperture above the atmosphere. Left - comparison between the expectation of the average realization presented in Fig. 10, combined with a model of the HET and atmosphere at AM=1.25, and the average measured throughput for 40 VIRUS units corrected for the field illumination of the WFC at center track. Right - measured throughputs for 40 VIRUS units (80 channels) showing the variation. The mean curve is shown in black and is the same as in the left panel, but extrapolated to 350 nm such that the average agrees. See text for details.

5.4 Early science commissioning

Figure 8, right, shows a typical observation with 39 units, obtained during early science observing for HETDEX. In the figure the wavelength dimension is collapsed so each IFU provides an image of the sky summed over 350-550 nm. Observation times per field are about 20 minutes for the HETDEX survey, split into three exposures of 360 seconds, and we expect to generate 40 TB of raw data over the course of the survey, including calibrations. In early science observing with VIRUS we have covered more than 3 sq. degrees of area at 1/4.5 fill factor, and detected more than 50k objects, a mix of LAEs, [OII] emitters and AGN. Current work is focused on understanding detection statistics utilizing observations of deep fields in the GOODS-N and COSMOS areas that have extensive ancillary data.

The ability to orchestrate the telescope control system has also led to improvements in efficiency. The Observing Conditions Decision (OCD) tool is a Python state machine that monitors the event stream from the metrology system to decide whether observing conditions are suitable for HETDEX observing. The HET system provides metrology events from the guiders that monitor the delivered image quality, transparency, and sky brightness for the facility. When conditions are suitable, OCD selects the best field and (if allowed) will automatically slew the telescope and perform the observation with only a minimal setup step needed from the Telescope Operator. Along with improvements in pointing, this orchestration has improved operational efficiency for HETDEX observing with VIRUS and is accomplished within a framework that will allow other instruments to interact with the telescope. The telescope points to <12 arcsec., 90% of the time, sufficient to place the guide stars on the guide probes without the additional step of setup with the acquisition camera, which saves time. Setup times are 5 minutes with a change in azimuth and 4 minutes without. The survey plan for HETDEX aims to keep the telescope at fixed azimuth (declination) for as many consecutive observations as possible to reduce overheads. While setup overheads have been driven down quite significantly during 2018, and meet requirements, we have not achieved the aggressive goal of achieving 1.5 minute setups for VIRUS observing when no azimuth change is required. Detailed examination of the events stream from the TCS will lead to further improvements. The consequence of missing the goal is a 7% increase in the 2200 hours of observing projected to complete HETDEX.

Parallel observations of VIRUS with LRS2 observations are routine. The instruments share the large rotary system shutter in the PFIP²¹, and both run with the CAMRA detector control software, so VIRUS data comes for free. The observations are not dithered, but are typically of much longer exposure time than the HETDEX observations, so have significant value for many projects. As the HET returns to full science operations in June 2018, VIRUS is also being made available for projects other than HETDEX from August 2018.



Replicable spectrographs like VIRUS and MUSE allow many different slicing modes between field and wavelength coverage/resolution, and these are discussed in Ref. 1. In that review we present Fig 12, following Bershadsky⁴³, which plots instrument areal grasp ($A\Omega$) versus spectral power (the product of the number of spectral resolution elements and the resolving power $N_\lambda R$, where $R = \lambda/\delta\lambda$ for wavelength λ and spectral resolution $\delta\lambda$) for survey instruments, and argue that the constraints of detector area and instrument size drive us into the replicated regime for survey instruments on the next generation of ELTs. The power of replication is illustrated in Fig. 12, VIRUS already has the highest grasp of any instrument and is unmatched for wide area blind spectroscopic surveys.

Figure 12: Performance metrics for VIRUS compared with other instruments, both existing and planned, after Ref. 1. Total Grasp is the product of telescope collecting area and area subtended by the sky spatial elements. Spectral Power is the product of the resolving power and the number of spectral resolution elements. Diagonal lines represent the loci of instruments with varying total detector pixel count. The grey shaded region is the zone of replicated instruments, as noted. Integral field spectrographs (IFS), high multiplex multi-object spectrographs (MOS) and replicated spectrographs are compared. The highly replicated instruments are emphasized by larger symbols. The location of the current deployment of 40 VIRUS units is noted.

6. SUMMARY

HETDEX consists of the HET WFU, VIRUS, and the blind spectroscopic survey of 420 sq. degrees. The HET Wide Field Upgrade is complete, with the widest field of view of any 10 m telescope and performance significantly improved over the original HET. Full science operations for the upgraded HET commenced in June 2018 (i.e. no engineering periods blocked out each month). VIRUS is now ~50% deployed, allowing us to advance and finalize all aspects of observing, data handling, and data analysis for the final instrument. It is already the highest grasp instrument in existence with 18,000 fibers on sky. HETDEX observing has started.

VIRUS provides a first and currently unique opportunity to understand the performance of spectrographs replicated on a 100-fold scale. Such instruments have applications on future extremely large telescopes. The experience with VIRUS is that it is possible to predict the performance and, with care in specifying component requirements, achieve the expectations

on-sky. When complete next year, the combination of the 10 m wide-field HET with the grasp of VIRUS, with 35,000 fibers on sky, will be a unique facility, able to survey vast areas of sky spectroscopically for the first time.

ACKNOWLEDGEMENTS

HETDEX is run by the University of Texas at Austin McDonald Observatory and Department of Astronomy with participation from the Ludwig-Maximilians-Universität München, Max-Planck-Institut für Extraterrestrische-Physik (MPE), Leibniz-Institut für Astrophysik Potsdam (AIP), Texas A&M University, Pennsylvania State University, Institut für Astrophysik Göttingen, University of Oxford and Max-Planck-Institut für Astrophysik (MPA). In addition to Institutional support, HETDEX is funded by the National Science Foundation (grant AST-0926815), the State of Texas, the US Air Force (AFRL FA9451-04-2-0355), by the Texas Norman Hackerman Advanced Research Program under grants 003658-0005-2006 and 003658-0295-2007, and by generous support from private individuals and foundations.

Financial support for innoFSPEC Potsdam of the German BMBF program *Unternehmen Region* (grant no. 03Z2AN11), and of Land Brandenburg, MWFK, is gratefully acknowledged. MMR also acknowledges support by the German BMI program *Wirtschaft trifft Wissenschaft*, grant no. 03WWBB105.

We thank the staffs of McDonald Observatory, HET, AIP, MPE, TAMU, IAG, Oxford University Department of Physics, the University of Texas Center for Electromechanics, and the University of Arizona College of Optical Sciences and Imaging Technology Lab for their contributions to the development of the WFU and VIRUS. Matthew Bershadsky kindly supplied his compilation of IFS characteristics used in Figure 12. We thank Chris Clemens and Jim Arns for helpful discussions during the development of the gratings for VIRUS, and Roger Smith and Ian McLean, for their assistance in reviewing the VIRUS detector system.

REFERENCES

- [1] Hill, G.J., “Replicated spectrographs in astronomy”, *Advanced Optical Technologies*. Vol 3, Issue 3, 265 (2014)
- [2] Hill, G.J., MacQueen, P.J., Palunas, P., Kelz, A., Roth, M.M., Gebhardt, K., and Grupp, F., “VIRUS: a hugely replicated integral field spectrograph for HETDEX”, *New Astronomy Reviews*, 50, 378 (2006)
- [3] Hill, G.J., MacQueen, P.J., Smith, M.P., Tufts, J.R., Roth, M.M., Kelz, A., Adams, J.J., Drory, N., Barnes, S.I., Blanc, G.A., Murphy, J.D., Gebhardt, K., Altmann, W., Wesley, G.L., Segura, P.R., Good, J.M., Booth, J.A., Bauer, S.-M., Goertz, J.A., Edmonston, R.D., and Wilkinson, C.P., “Design, construction, and performance of VIRUS-P: the prototype of a highly replicated integral-field spectrograph for HET”, *Proc. SPIE*, 7014-257 (2008)
- [4] Hill, G.J., Gebhardt, K., Komatsu, E., Drory, N., MacQueen, P.J., Adams, J.A., Blanc, G.A., Koehler, R., Rafal, Roth, M.M., Kelz, A., Grupp, F., Murphy, J., Palunas, P., Gronwall, C., Ciardullo, R., Bender, R., Hopp, U., and Schneider, D.P., “The Hobby-Eberly Telescope Dark Energy Experiment (HETDEX): Description and Early Pilot Survey Results”, in *Panoramic Views of the Universe*, ASP Conf. Series, 399, 115 (2008)
- [5] Hill, G.J., Cornell, M.E., DePoy, D.L., Drory, N., Fabricius, M.H., Kelz, A., Lee, H., Marshall, J.L., Murphy, J.D., Prochaska, T., Tuttle, S.E., Vattiat, B.L., Allen, R.D., Blanc, G., Chonis, T.S., Gebhardt, K., Good, J.M., Haynes, D.M., MacQueen, P.J., Rafal, M.D., Roth, M.M., Savage, R.D., and Snigula, J.M., “VIRUS: production of a massively replicated fiber integral field spectrograph for the upgraded Hobby-Eberly Telescope,” *Proc. SPIE*, 8446-21 (2012)
- [6] Kelz, A., Jahn, T., Haynes, D.M., Hill, G.J., Murphy, J.D., Rutowska, M., Streicher, O., Neumann, J., Nicklas, N., Sandin, C., Fabricius, M., “HETDEX / VIRUS: testing and performance of 33,000 optical fibres”, *Proc. SPIE*, 9147-269 (2014)
- [7] Hill, G.J., Tuttle, S.E., Vattiat, B.L., Lee, H., Drory, N., Kelz, A., Ramsey, J., DePoy, D.L., Marshall, J.L., Gebhardt, K., Chonis, T.S., Dalton, G.B., Farrow, D., Good, J.M., Haynes, D.M., Indahl, B.L., Jahn, T., Kriel, H., Montesano, F., Nicklas, H., Noyola, E., Prochaska, T., Allen, R.D., Blanc, G., Fabricius, M.H., Landriau, M., MacQueen, P.J., Roth, M.M., Savage, R., Snigula, J.M., “VIRUS: first deployment of the massively replicated fiber integral field spectrograph for the upgraded Hobby-Eberly Telescope”, *Proc. SPIE*, 9908-54 (2016)
- [8] Hill, G.J., “HETDEX and VIRUS: Panoramic Integral Field Spectroscopy with 35k fibres” in ‘Multi-Object Spectroscopy in the Next Decade’ a conference held in La Palma, March 2015, (eds. I. Skillen, M. Balcells & S. Trager), ASP Conference Series, 507, 393 (2016)
- [9] Vattiat, B.L., Hill, G.J., Kelz, A., Martin, J., Mrozinski, E., Jahn, T., Spencer, R., “Deployment and handling of the VIRUS fiber integral field units”, 10702-303 (2018)

- [10] Lee, H., Vattiat, B.L., Hill, G.J., "Efficient high-precision CCD-field lens alignment and integration process of mass-produced fast astronomical spectrograph cameras with VIRUS as an example", 10706-55 (2018)
- [11] Spencer, R., Balderrama, E., Damm, G., Fowler, J., Good, J., Hill, G.J., Kriel, H., MacQueen, P.J., Mrozinski, E., Perry, D., Peterson, T., Shetrone, M., Savage, R., Cook, E., Smith, G., DePoy, D.L., Marshall, J.M., Prochaska, T., Saucedo, M., "VIRUS: the instrument infrastructure to support the deployment and upkeep of 156 spectrographs at the Hobby-Eberly telescope", 10706-246 (2018)
- [12] Hill, G.J., Drory, N., Good, J., Lee, H., Vattiat, B.L., Kriel, H., Bryant, R., Elliot, L., Landiau, M., Leck, R., Perry, D., Ramsey, J., Savage, R., Damm, G., Fowler, J., Gebhardt, K., MacQueen, P.J., Martin, J., Ramsey, L.W., Shetrone, M., Schroeder, E., Cornell, M.E., Booth, J.A., and Moriera, W., "Deployment of the Hobby-Eberly Telescope Wide Field Upgrade", Proc. SPIE, 9145-5 (2014)
- [13] John M. Good, Gary J. Hill, Martin Landiau, Hanshin Lee, Emily Schroeder-Mrozinski, Jerry Martin, Herman Kriel, Matthew Shetrone, James Fowler, Richard Savage, Ron Leck, "HET Wide Field Upgrade Tracker System Performance", Proc. SPIE 9906-167 (2016)
- [14] Hill, G.J., Drory, N., Good, J.M., Lee, H., Vattiat, B.L., Kriel, H., Ramsey, J., Randy Bryant, R., Elliot, L., Fowler, J., Landiau, M., Leck, R., Odewahn, S., Perry, D., Savage, R., Schroeder Mrozinski, E., Shetrone, M., Damm, G., Gebhardt, K., MacQueen, P.J., Martin, J., Armandroff, T., Ramsey, L.W., "The Hobby-Eberly Telescope wide-field upgrade", Proc. SPIE 9906-5 (2016)
- [15] Hill, G.J., Drory, N., Good, J.M., Lee, H., Vattiat, B.L., Kriel, H., Ramsey, J., Bryant, R., Fowler, J.R., Landiau, M., Leck, R., Mrozinski, E., Odewahn, S., Shetrone, M., Westfall, A., Terrazas, E., Balderrama, E., Buetow, B., Damm, G., MacQueen, P.J., Martin, J., Martin, A., Smither, K., Rostopchin, S., Smith, G., Spencer, R., Armandroff, T., Gebhardt, K., Ramsey, L.W., "Completion and performance of the Hobby-Eberly telescope wide field upgrade", Proc. SPIE, 10700-20 (2018)
- [16] Lee, H., Hill, G.J., Drory, N., Vattiat, B.L., Ramsey, J., Bryant, R., Shetrone, M., Odewahn, S., Rostopchin, S., Landiau, M., Fowler, J., Leck, R., Kriel, H., Damm, G., "New Hobby Eberly telescope metrology systems: design, implementation, and on-sky performance", 10700-78 (2018)
- [17] Good, J.M., Leck, R., Ramsey, J., Drory, N., Hill, G.J., Fowler, J.R., Kriel, H., Landiau, M., "Mechanical systems performance of the HET wide-field upgrade", 10700-143 (2018)
- [18] Bacon, R., Accardo, M., Adjali, L., Anwand, H., Bauer, S., *et al.*, "The second-generation VLT instrument MUSE", Proc. SPIE 7735, 773508 (2010)
- [19] Lee, H., Hill, G.J., Good, J.M., Vattiat, B.L., Shetrone, M., Martin, J., Schroeder Mrozinski, E., Kriel, H., Oh, C.-J., Frater, E., Smith, B., Burge, J.H., "Delivery, installation, on-sky verification of Hobby Eberly Telescope wide-field corrector," Proc. SPIE 9906-156 (2016)
- [20] Vattiat, B.L., *et al.*, "Design, testing, and performance of the Hobby Eberly Telescope prime focus instrument package," Proc. SPIE, 8446-269 (2012)
- [21] Vattiat, B.L., Hill, G.J., Lee, H., Moreira, W., Drory, N., Ramsey, J., Elliot, L., Landiau, M., Perry, D.M., Savage, R., Kriel, H., Haeuser, M., and Mangold, F., "Design, alignment, and deployment of the Hobby Eberly Telescope prime focus instrument package", Proc. SPIE, 9147-172 (2014)
- [22] Ramsey, J., Drory, N., Bryant, R., Elliott, L., Fowler, J., Hill, G. J., Landiau, M., Leck, R., Vattiat, B., "A control system framework for the Hobby-Eberly Telescope", Proc. SPIE, 9913-160 (2016)
- [23] Tuttle, S.E., Hill, G.J., Lee, H., Vattiat, B.L., Noyola, E., Drory, N., Cornell, M.E., Peterson, T., Chonis, T.S., Allen, R.D., Dalton, G.B., DePoy, D.L., Edmonston, R.D., Fabricius, M.H., Kelz, A., Haynes, D.M., Landiau, M., Lesser, M.P., Leach, R.W., Marshall, J.L., Murphy, J.D., Perry, D., Prochaska, T., Ramsey, J., and Savage, R., "The construction, alignment, and installation of the VIRUS spectrograph", Proc. SPIE 9147-26 (2014)
- [24] Marshall, J. L., DePoy, D. L., Prochaska, T., Allen, R. D., Williams, P., Rheault, J. P., Li, T., Nagasawa, D. Q., Akers, C., Baker, D., Boster, E., Campbell, C., Cook, E., Elder, A., Gary, A., Glover, J., James, M., Martin, E., Meador, W., Mondrik, N., Rodriguez-Patino, M., Villanueva, Jr., S., Hill, G. J., Tuttle, S., Vattiat, B., Lee, H., Chonis, T. S., Dalton, G. B., and Tacon, M., "VIRUS instrument collimator assembly," Proc. SPIE 9147-143 (2014)
- [25] H. Lee, *et al.*, "VIRUS optical tolerance and production," Proc. SPIE, 7735-140 (2010)
- [26] Chonis, T.S., Hill, G.J., Clemens, J.C., Dunlap, B., and Lee, H., "Methods for evaluating the performance of volume phase holographic gratings for the VIRUS spectrograph array," Proc. SPIE, 8446-209 (2012)
- [27] Chonis, T. S., Frantz, A., Hill, G. J., Clemens, J. C., Lee, H., Adams, J. J., Marshall, J. L., DePoy, D. L., and Prochaska, T., "Mass production of volume phase holographic gratings for the VIRUS spectrograph array," Proc. SPIE 9151-53 (2014)

- [28] Burgh, E.B., Bershad, M.A., Westfall, K.B., and Nordsieck, K.H., "Recombination Ghosts in Littrow Configuration: Implications for Spectrographs Using Volume Phase Holographic Gratings," *PASP* 119, 1069 (2007)
- [29] Murphy, J.D., Palunas, P., Grupp, F., McQueen, P.J., Hill, G.J., Kelz, A., and Roth, M.M., "Focal ratio degradation and transmission in VIRUS-P optical fibers," *Proc. SPIE*, 7018-104 (2008)
- [30] Murphy, J.D., *et al.*, "The Effects of Motion and Stress on Optical Fibers", *Proc. SPIE*, 8446-207 (2012)
- [31] Snigula, J. M., Drory, N., Fabricius, M., Landriau, M., Montesano, F., Hill, G. J., Gebhardt, K., Cornell, M. E., "Cure-WISE: HETDEX Data Reduction with Astro-WISE", *ASP Conf. Series*, 485, 447 (2014)
- [32] Smith, M.P., Mulholland, G.T., Booth, J.A., Good, J.M., Hill, G.J., MacQueen, P.J., Rafal, M.D., Savage, R.D., and Vattiat, B.L., "The cryogenic system for the VIRUS array of spectrographs on the Hobby Eberly Telescope", *Proc. SPIE*, 7018-117 (2008)
- [33] Chonis, T.S., *et al.*, "Development of a cryogenic system for the VIRUS array of 150 spectrographs for the Hobby-Eberly Telescope," *Proc. SPIE*, 7735-265 (2010)
- [34] Reiss, R., Deiries, S., Lizon, J.-L., and Rupprecht, G., "The MUSE instrument detector system", *Proc. SPIE* 8446, 84462P (2012)
- [35] Lee, H., and Hill, G.J., "Image moment-based wavefront sensing for in-situ full-field image quality assessment," *Proc. SPIE*, 8450-191 (2012)
- [36] Lee, H., Hill, G.J., Tuttle, S.E., and Vattiat, B.L., "Fine optical alignment correction of astronomical spectrographs via in-situ full-field moment-based wavefront sensing," *Proc. SPIE*, 8450-192 (2012)
- [37] Indahl, B., Hill, G. J., Drory, N., Gebhardt, K., Tuttle, S., Ramsey, J., Ziemann, G., Chonis, T., Peterson, T., Peterson, A., Vattiat, B., Li, H., Hao, L., "VIRUS Characterization Development and Results from First Batches of Delivered Units", *Proc. SPIE*, 9908-299 (2016)
- [38] Indahl, B.L., Hill, G. J., Ziemann, G., Froning, C., Gebhardt, K., Kelz, A., Jahn, T., Montesano, F., Sinigula, J., MacQueen, P.J., Peterson, T., Drory, N., Chonis, T., Lee, H., Vattiat, B., Ramsey, J., Peterson, A., "VIRUS: comparison of lab characterization with on-sky performance for multiple spectrograph units", *Proc. SPIE* 10702-294 (2018)
- [39] Prochaska, T., Allen, R., Rheault, J. P., Cook, E., Baker, D., DePoy, D. L., Marshall, J. L., Hill, G.J., and Perry, D., "VIRUS instrument enclosures," *Proc. SPIE* 9147-257 (2014)
- [40] Tuttle, S.E., Hill, G. J., Vattiat, B. L., Lee, H., Drory, N., Kelz, A., Ramsey, J., Peterson, T., Noyola, E., DePoy, D. L., Marshall, J. L., Chonis, T. S., Dalton, G.B., Fabricius, M. H., Farrow, D., Good, J. M., Haynes, D. M., Indahl, B., Jahn, T., Kriel, H., Nicklas, H., Montesano, F., Prochaska, T., Allen, R. D., Landriau, M., MacQueen, P. J., Roth, M. M., Savage, R., Snigula, J. M. , "VIRUS early installation and commissioning.", *Proc SPIE* 9908-55 (2016)
- [41] Chonis, T.S., Hill, G.J., Lee, H., Tuttle, S.E., Vattiat, B.L., Drory, N., Indahl, B.L., Peterson, T.W., Ramsey, J., "LRS2 – design, assembly, testing, and commissioning of the second generation low resolution spectrograph for the Hobby-Eberly Telescope", *Proc. SPIE* 9908-163 (2016)
- [42] Mahadevan, S., *et al.*, "The habitable-zone planet finder: engineering and commissioning on the Hobby Eberly telescope," *Proc. SPIE* 10702-40 (2018)
- [43] Bershad, M.A., "3D Spectroscopic Instrumentation" in '3D Spectroscopy in Astronomy, XVII Canary Island Winter School of Astrophysics', Cambridge University Press, Cambridge, (2009)